Journal of Peptide Science
J. Peptide Sci. **5**: 410–422 (1999)

Solution Structure of Human β-endorphin in Helicogenic solvents: an NMR Study

GABRIELLA SAVIANO[a], ORLANDO CRESCENZI[b], DELIA PICONE[b], PIERANDREA TEMUSSI[c,1] and TEODORICO TANCREDI[d,*]

[a] Università del Molise, Isernia, Italy
[b] Dipartimento di Chimica, Università di Napoli Federico II, Napoli, Italy
[c] Division of Molecular Structure, NIMR, MRC, Mill Hill, London, UK
[d] Istituto Chimica MIB del CNR, associated with the National Institute for the Chemistry of Biological Systems, via Toiano 6, Arco Felice, Napoli, Italy

Received 3 May 1999
Accepted 20 May 1999

Abstract: β-Endorphin is the largest natural opioid peptide. The knowledge of its bioactive conformation might be very important for the indirect mapping of the active site of opioid receptors. We have studied β-endorphin in a variety of solution conditions with the goal of testing the intrinsic tendency of its sequence to assume a regular fold. We ran NMR experiments in water, dimethylsulfoxide and aqueous mixtures of methanol, ethylene glycol, trifluoroethanol, hexafluoracetone trihydrate and dimethylsulfoxide. The solvent in which the peptide is more ordered is the hexafluoracetone trihydrate/water mixture. The helical structure detected for β-endorphin in this mixture at 300 K extends for the greater part of its address domain, hinting at a possible mechanism of interaction with opioid receptors: a two-point attachment involving an interaction of the helical part of the address domain (PLVTLFKNAIIKNAY) with one of the transmembrane helices and a classical interaction of the message domain (YGGF) with the receptor subsite common to all opioid receptors. Copyright © 1999 European Peptide Society and John Wiley & Sons, Ltd.

Keywords: β-endorphin; opioid peptides; NMR structure; solvent scan; linear peptides

INTRODUCTION

Human β-endorphin is an endogenous opioid peptide [1,2] corresponding to the 237–267 *C*-terminal fragment of proopiomelanocortin [3]. If one subdivides the sequence of β-endorphin (YGGFMTSEKS[10]QTPLVTLFKN[20]AIIKNAYKKG[30]E) in two functional domains, the recognition or message domain and the address domain according to Schwyzer [4], it is easy to locate the message domain in the *N*-terminal part of the sequence (YGGF). It coincides with the corresponding domains of most natural and synthetic opioid peptides [5], in particular enkephalins [6] and dynorphins [7], with the obvious exceptions of β-casomorphin [8], endomorphins [9], dermorphin and deltorphins [10]. Accordingly, it is not surprising that β-endorphin has an opioid activity similar to those of enkephalins [6] and dynorphins [7], the original endogenous opioids, i.e. it interacts with μ (MOR), δ (DOR) and κ (KOR) receptors with little selectivity [11–13].

Abbreviations: CD, circular dichroism; CIDNP, chemically induced dynamic nuclear polarization; DAMGO, [D-Ala2-*N*-MePhe4,Gly-ol5]enkephalin; DMSO, perdeuterated dimethylsulfoxide; DOR, δ opioid receptor; DQF-COSY, double-quantum filtered correlation spectroscopy; EG, ethylene glycol; HFA, hexafluoracetone trihydrate; KOR, κ opioid receptor; MD, molecular dynamics; MM, molecular mechanics; MOR, μ opioid receptor; NMR, nuclear magnetic resonance; NOE, nuclear Overhauser effect; NOESY, nuclear Overhauser effect spectroscopy; TAD, torsion angle dynamics; TFE, trifluoroethanol; TM, trans membrane; TOCSY, total correlation spectroscopy; TPPI, time proportional phase incrementation.

* Correspondence to: Istituto Chimica MIB del CNR, via Toiano 6, 80072 Arco Felice, Napoli, Italy. E-mail: teo@nmr.icmib.na.cnr.it
[1] On leave of absence from Dipartimento di Chimica, Università Federico II, Napoli, Italy.

CCC 1075–2617/99/090410-13$17.50

It had been proposed that β-endorphin interacts with a fourth highly specific receptor, the ε receptor of the mouse vas deferens [14–16], possibly present in the brain of guinea pig, cow, chicken as well as pig [17]. However, contrary to MOR, DOR and KOR, that have been repeatedly identified in several organisms during the last few years [18], no sequence corresponding to the ε receptor has yet been reported. There are, however, indications that the interaction of β-endorphin with opioid receptors may be anyway different from those of other agonists. It has been recently shown that β-endorphin binds to sites in the rat caudal dorsomedial medulla, corresponding to μ-opioid receptors, with a relative potency higher than those of DAMGO and naloxone [19] and that single-nucleotide polymorphism in the human μ opioid receptor gene can alter significantly β-endorphin binding and activity [20].

β-endorphin is characterized by the longest sequence among natural opioid peptides that, typically, have from four (morphiceptin) to seven (deltorphins) residues [21]. This feature increases the interest for its conformation since its longer sequence (corresponding to a larger volume) and the possible presence of additional interaction points might be important for the indirect mapping of the active site of opioid receptors. In this connection it is interesting that specific stimulation of phosphorylation of MOR by β-endorphin hints the existence of different agonist-dependent conformations of MOR [22]. However, the structural features of this peptide have been studied less than those of other endogenous opioids. Most early studies, both experimental [23–33] and predictive [25,27] pointed to the presence of helical segments but failed to identify a consensus helical stretch. CD spectroscopy studies in water found no significant sign of secondary structure [23] but studies in alcohol–water mixtures [23–27] or micelles [24,27,31] indicated a helical content varying from 0 to 50%. Previous conformational analyses of β-endorphin based on NMR include a study in water consistent with an essentially random coil conformation [28], a photo-CIDNP study in an aqueous solution of phospholipid micelles [29,30] that revealed limited accessibility of Tyr-27 and a study in a mixture of methanol and water (60:40, v/v) that identified two long helical stretches encompassing nearly the entire length of the molecule: between residues 1 and 12 and between residues 14 and 28 [33]. This last structure is very surprising since the first five residues, corresponding to the sequence of Met-enkephalin, have never been found ordered in solution in any of the numerous peptides to which they confer opioid activity [21]. However, none of the experimental studies yielded a detailed structural model. Even the most recent one [33] was only qualitative since, owing to resonance superpositions and the very poor quality of the spectra, nearly all NOEs used to identify the structure were unassigned NOEs.

Without a detailed molecular model of β-endorphin it is not possible to propose mechanisms of interaction with opioid receptors that go beyond the conformational preferences of the message domain, thoroughly explored for enkephalins and some of their synthetic analogs [34]. Therefore, we have undertaken a systematic investigation of the conformational state of β-endorphin in several solvents, representative of either transport fluids or of the less polar environments presumed for the interior of a typical G protein-coupled receptor [35].

Here we report results from NMR experiments in two neat solvents, water and DMSO, and in aqueous mixtures of methanol, EG, TFE, HFA and DMSO.

MATERIALS AND METHODS

Sample Preparation

Human β-endorphin was purchased from Bachem Inc. (Torrance, CA, USA). The amino acid analysis was satisfactory. The purity of the peptide sample is better than 99% as judged from a HPLC run on a Vydac C-18 column eluted with linear gradient H_2O 0.1% TFA and CH_3CN 0.1% TFA. As a further check, all resonances in the NMR spectra are attributable to protons of the β-endorphin. Hexafluoroacetone trihydrate (HFA) was obtained from Fluka Chemie AG (Buchs, Switzerland). $DMSO_{d6}$, $methanol_{d4}$, EG_{d4}, TFE_{d3} and deuterated HFA were purchased from Cambridge Isotope Labs (Andover, MA, USA). NMR samples were prepared by dissolving appropriate amounts of peptide in 0.5 ml of solvent to make approximately 1 mM solutions.

NMR Measurements

Proton NMR spectra were run on Bruker DRX-400 and on Bruker DRX-500 spectrometers. A conventional set of 2D spectra, according to the scheme of sequential assignment described by Wüthrich [36] was recorded: DQF-COSY [37], TOCSY [38] and NOESY [39]. Total correlated spectroscopy (TOCSY)

spectra were collected with mixing times in the range 50–75 ms, using the clean MLEV-17 mixing scheme [40]. The nuclear Overhauser enhancement spectroscopy (NOESY) spectra were recorded with mixing times of 50, 100 and 200 ms. TPPI was applied to achieve quadrature detection in the virtual dimension [41]. Water suppression was achieved either by presaturation or by using the WATERGATE pulse sequence [42].

Slowly exchanging amide protons of β-endorphin were detected by a series of 1D and NOESY experiments. 1D spectra were recorded systematically in a time interval of 4300 min after the sample was dissolved in the appropriate mixture of D_2O and perdeuterated HFA. Control NOESY spectra were collected at 15 and 1400 min after dissolution.

Data processing was performed with standard Bruker software (XwinNMR and AURELIA).

Structure Calculation

The input data for the structure calculation with the program DYANA [43] were generated from the peak volumes obtained from AURELIA. Figure 1 summarizes all measured NOEs, classified as intraresidue, sequential and medium range ($1 < |i-j| \leq 5$).

Based on the peak volumes observed on the NOESY spectra, the upper distance limits were generated with the program CALIBA [43]. Further restraints corresponding to hydrogen bonds were introduced after H/D exchange experiments. Computations were performed on SGI O2 computers. During the DYANA calculation using the simulated annealing protocol in torsion angle space, we introduced all available restraints. In the final refinement step, these restraints were converted to the input data format used in the AMBER program [44,45] and used to perform both restrained MM and restrained MD. In this refinement a standard simulated annealing protocol in Cartesian space was applied to finally obtain an ensemble of structures having no violation greater than 0.5 Å in distance from the input restraints. The AMBER calculation was also performed on SGI O2 computers.

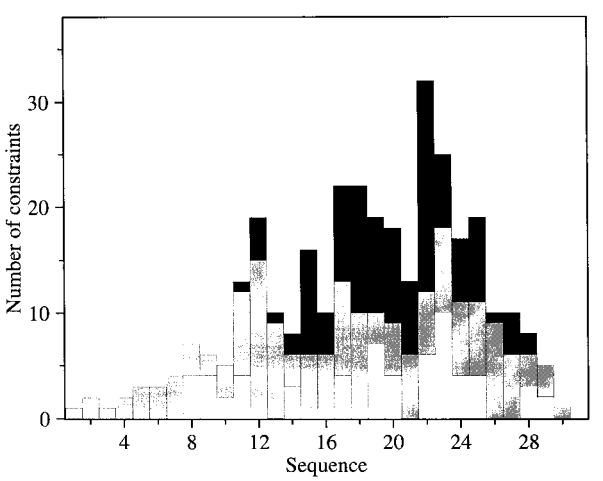

Figure 1 Number of NOEs versus residue number for β-endorphin in HFA/water (50:50, v/v). Intraresidue effects are shown as white bars, sequential as gray bars and medium-range ($1 < |i-j| \leq 5$) as black bars.

The 20 DYANA structures with the lowest target function values were subjected to multiple restrained annealings using the SANDER module of AMBER 5.0 package. The 1991 version of the all-atom force field was used [44], with a distance-dependent dielectric constant $\varepsilon = r_{ij}$. In order to reduce the artifacts which can arise during *in vacuo* simulation, the charge of the ionizable groups was reduced to 20% of its full value. A distance cutoff of 12 Å was used in the evaluation of nonbonded interactions. Distance restraints were applied as a flat well with parabolic penalty within 0.5 Å outside the upper bound, and a linear function beyond 0.5 Å, using a force constant of 16 kcal mol^{-1} $Å^{-2}$. No hydrogen bond restraints were used during this phase of the refinement.

The simulated annealing protocol was as follows. First, each structure was minimized in the presence of NMR restraints with 200 steps of the steepest descent algorithm, followed by 800 steps of conjugate gradient algorithm. This was followed by a simulated annealing cycle of 20 ps, with temperature coupling to an external bath [46], and using a time step of 1 fs: (i) the system was kept at 1 K during 2 ps with a temperature relaxation time (τ) of 0.05 ps; the restraint force constant was increased linearly from 0 to 16 kcal mol^{-1} $Å^{-2}$ during the first 1 ps; (ii) heating to 500 K in 2 ps with τ increasing linearly from 0.05 to 0.1 ps; (iii) equilibration at 500 K during 4 ps with $\tau = 0.1$ ps; (iv) slow cooling during 12 ps with a target temperature of 0 K. The cooling schedule used τ from 2.0 to 1.0 in 8 ps; $\tau = 0.5$ during 2 ps; $\tau = 0.2$ during 1 ps; $\tau = 0.05$ during the last 1 ps.

The whole annealing cycle was repeated several times from each starting, energy-minimized structure: one run used initial atom velocities computed from forces, while seven more runs were started with different random Boltzman distribution of atom velocities (at $T = 1$ K).

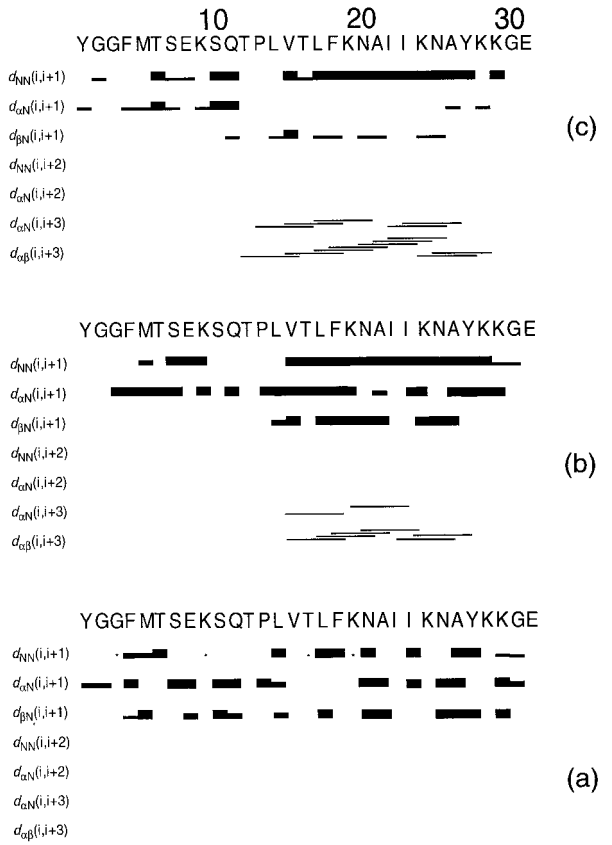

Figure 2 Summary of diagnostic NOEs of β-endorphin involving backbone NH and H^{α} atoms. (a) 80:20 (v/v) DMSO/water cryomixture, (b) 30:70 (v/v) TFE/water mixture and (c) 50:50 (v/v) HFA/water mixture.

The best ten structures, having residual restraint energies of less than 17 kcal mol^{-1}, were selected to represent the solution structure.

To display the final structures, calculations of the mean coordinates of the ensemble structures and their r.m.s.d. values were carried out with the program MOLMOL [47].

RESULTS

Environment Selection

β-Endorphin was examined in a variety of solvents, ranging from the polar media typical of the transport fluids to less polar environments resembling the active sites of many receptors. Assignment of proton resonances in all solvents was facilitated by the similarity of the spectra but was performed anew for each solvent in the conventional manner by the standard protocol [36] based on the use of DQF-COSY, TOCSY and NOESY spectra.

We have shown that it may be possible to influence the conformational equilibria of short peptides and even of flexible regions of proteins by an appropriate choice of the environment, i.e. by the use of what can be termed 'environmental constraints' [48–50]. The measurement of NOEs and, to some extent, even the conformation of short linear peptides in solution can be influenced by the use of cryoprotective mixtures [51], i.e. solvent mixtures of viscosity higher than that of pure water but comparable to that of cytoplasm [52]. These media can actually play the role of effective 'environmental constraints' since they act as conformational sieves that can select ordered, more compact conformers with respect to extended and/or disordered ones. However, spectra in water, DMSO and in a mixture of water with DMSO (20:80, v/v), show little ordering of the peptide. Figure 2 shows a comparison of the bar diagrams of β-endorphin in a DMSO/water cryomixture (80:20, v/v), a TFE/water mixture (30:70, v/v) and a HFA/water mixture (50:50, v/v). Even if the NOESY spectrum in the cryomixture is richer than that in other polar solvents, the number of diagnostic NOEs is not sufficient to define a single ordered structure. On the contrary, all media that are known to favor helical conformations show rich NOESY spectra consistent with a high helical content. Alcohols, either neat or mixed with water are the most popular media used to induce helicity in

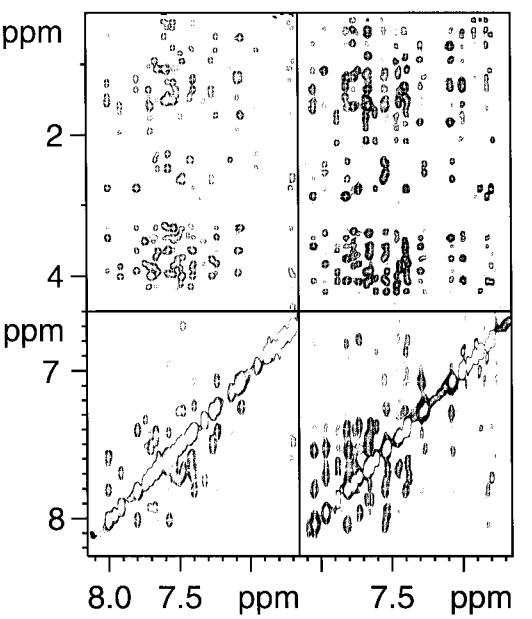

Figure 3 Comparison of partial 500 MHz NOESY spectra of β-endorphin recorded at 300 K in 30:70 (v/v) TFE/water (left) and 50:50 (v/v) HFA/water (right).

Table 1 Proton Chemical Shifts (ppm) of 1 mM Human β-Endorphin in 50:50 (v/v) HFA/H_2O at 300 K

	NH	α	β–β'	γ–γ'	δ–δ'	ε–ε'
Tyr^{1}	—	3.848	2.780		6.797	6.530
Gly^{2}	7.760	3.650–3.505				
Gly^{3}	7.394	3.567				
Phe^{4}	7.388	4.209	2.764		6.980	6.872
Met^{5}	7.602	4.032	1.664	2.079		
Thr^{6}	7.383	3.960	3.960	0.880		
Ser^{7}	7.640	4.075	3.642–3.567			
Glu^{8}	7.873	3.939	1.770–1.704	2.105		
Lys^{9}	7.672	3.936	1.554–1.470	1.140	1.351	2.656
Ser^{10}	7.525	4.080	3.642–3.569			
Gln^{11}	7.664	4.130	1.889–1.725	2.068		6.781–6.187
Thr^{12}	7.455	4.217	4.000	0.957		
Pro^{13}		4.060	1.717–1.565	2.040	3.481–3.393	
Leu^{14}	6.990	3.749	1.254	1.320	0.599–0.529	
Val^{15}	7.075	3.459	1.816	0.738–0.711		
Thr^{16}	7.287	3.928–3.580	3.928	0.925		
Leu^{17}	7.396	3.754	1.308	1.455	0.540–0.489	
Phe^{18}	7.811	4.067	2.871		6.980	6.821
Lys^{19}	8.041	3.577	1.610–1.549	1.086	1.348	2.606
Asn^{20}	7.544	4.038	2.625–2.386		7.067–6.283	
Ala^{21}	7.801	3.741	1.185			
Ile^{22}	7.758	3.362	1.592	1.169–0.692, 0.497 (Me)	0.363	
Ile^{23}	7.651	3.401	1.573	1.340–0.869, 0.567 (Me)	0.494	
Lys^{24}	7.645	3.692	1.566	1.091	1.343–1.236	2.651
Asn^{25}	7.538	4.220	2.539–2.416		7.257–6.283	
Ala^{26}	7.958	3.826	1.086			
Tyr^{27}	7.723	4.078	2.772		6.790	6.460
Lys^{28}	7.375	3.829	1.504	1.067	1.348	2.670
Lys^{29}	7.434	3.923	1.501	1.153	1.356	2.680
Gly^{30}	7.653	3.505				
Glu^{31}	7.386	3.987	1.835–1.648	2.084		

The values are referred to residual HDO peak at 4.700 ppm.

peptides [53–57]. In addition to the quoted mixture of methanol and water employed by Lichtarge *et al.* [33], we ran spectra of β-endorphin in mixtures of water with EG, TFE and HFA. This last mixture has been recently shown to behave like TFE/water mixtures but with a much higher helix-inducing propensity [58].

Resonance Assignments and Secondary Structure

Figure 3 shows the comparison of partial 500 MHz NOESY spectra of β-endorphin in TFE/water (30:70, v/v) and HFA/water (50:50, v/v) at 300 K. The spectra are rather similar and show features typical of helical structures, e.g. the presence of many NH–NH cross peaks. The data in HFA/water (50:50, v/v) are of better quality than those in TFE/water (30:70, v/v) and were accordingly used for a quantitative structure determination. Table 1 shows the proton chemical shifts, referred to the residual HDO peak at 4.700 ppm. Inspection of the NOEs in HFA/water (50:50, v/v) shows that those of the *N*-terminal part are similar to the ones previously observed for Leu-enkephalin [21,59]. That is, the *N*-terminal part of the peptide lacks 'medium range' NOEs but is characterized by a series of sequential NH–NH effects consistent with a mixture of poorly structured conformers. On the other hand, for resonances assigned to protons belonging to residues from Pro^{13} to Tyr^{27} it was possible to observe several 'medium range' NOEs suggesting the presence of a regular structured conformer. Particularly, diagnostic $d_{\alpha N}(i, i+3)$ and $d_{\alpha\beta}(i, i+3)$ effects hint the presence in this segment of an α-helix. Figure 2 summarizes

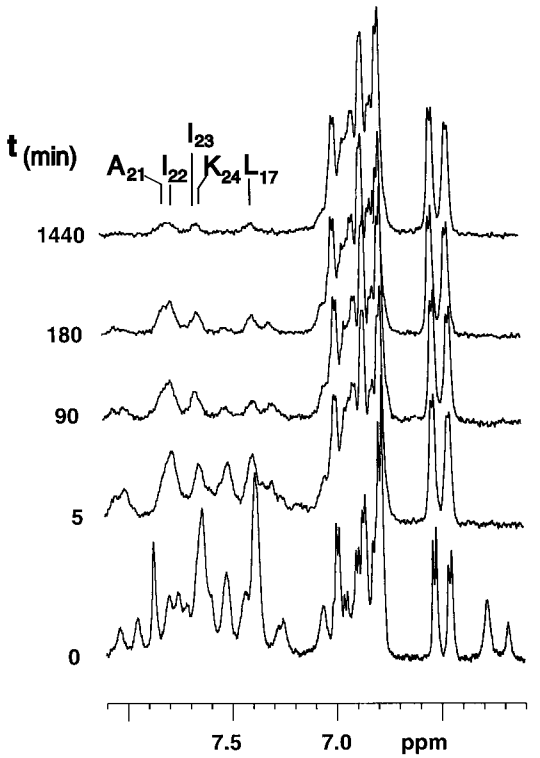

Figure 4 Hydrogen/deuterium exchange of β-endorphin dissolved in deuterated 50:50 (v/v) HFA/D_2O. The partial 500 MHz 1D spectra at 300 K are shown as a function of time after dissolution (min); the spectrum labeled 0 is a reference 1D spectrum in HFA/H_2O (50:50, v/v). NH resonances with highest half-lives (of L^{17}, A^{21}, I^{22}, I^{23} and K^{24}) are explicitly indicated.

diagnostic NOEs in HFA/water (50:50, v/v). All data are consistent with a helical segment in the *C*-terminal (address) moiety.

Structure Determination

Introduction of restraints derived from intraresidue, sequential and medium range NOEs in DYANA [43] generated 20 structures of β-endorphin with good values of the usual target function [43] out of 50 random generated initial conformers. All 20 structures have similar values of the backbone torsion angles for the *C*-terminal part but diverge in the *N*-terminal region. The whole sequence from Pro^{13} to Tyr^{27} is a fairly regular α helix. Small deviations from a canonical α-helical structure may originate from an insufficient number of constraints in the refinement procedure. Accordingly we tried to introduce further constraints derived either from coupling constants or hydrogen bonds.

The linewidth of the resonances in HFA/water (50:50, v/v) prevented accurate direct measurements of coupling constants. We did try to evaluate $J_{\alpha HNH}$ values by means of the method of Kim and Prestegard [60] that is based on measurement of separations of extrema in dispersive and absorptive COSY spectra. The quality of the results however, was not sufficient to introduce angle constraints in the DYANA runs. Indications of the likely presence of hydrogen bonds could be inferred from the recurrence of short O–N distances in all 20 structures generated by DYANA but data from the calculation protocol cannot be used blindly without risking a vicious circle. In order to avoid arbitrary solutions we tried to find experimental evidence for hydrogen bonds. Amide hydrogens involved in intramolecular hydrogen bonding or otherwise shielded from solvent, can be identified by their relatively slow rate of H/D exchange. Obtaining this information is commonplace in structural determinations of proteins but is generally very difficult in small peptides whose amide hydrogens normally exchange very fast with deuterated solvents containing labile deuterons. Even peptides that exist as isolated small stretches of canonical secondary structures in solution generally do not show slow H/D exchange. However, one of the few experimental examples, i.e. a comparative study of temperature

Table 2 Summary of Residual Constraint Violations (*d*) and Energies (*E*)

d range (Å)	Average no. of *d* violations	Energy term	Average AMBER *E* (kcal mol^{-1})
$0.1 < d \leq 0.2$	12.9 ± 2.9	*E* (distance constraint)	14.83 ± 1.20
$0.2 < d \leq 0.3$	5.0 ± 1.3	*E* (Van der Waals)	-94.41 ± 6.85
$0.3 < d \leq 0.4$	2.0 ± 1.0	*E* (total)	-276.58 ± 18.41
$0.4 < d \leq 0.5$	0.2 ± 0.4		
$0.5 < d$	0		

Average maximum violation (Å) 0.38 ± 0.04.
The force constants for the distance constraints were16 kcal mol^{-2} $Å^{-2}$.
The errors are given as ± 1 SD.

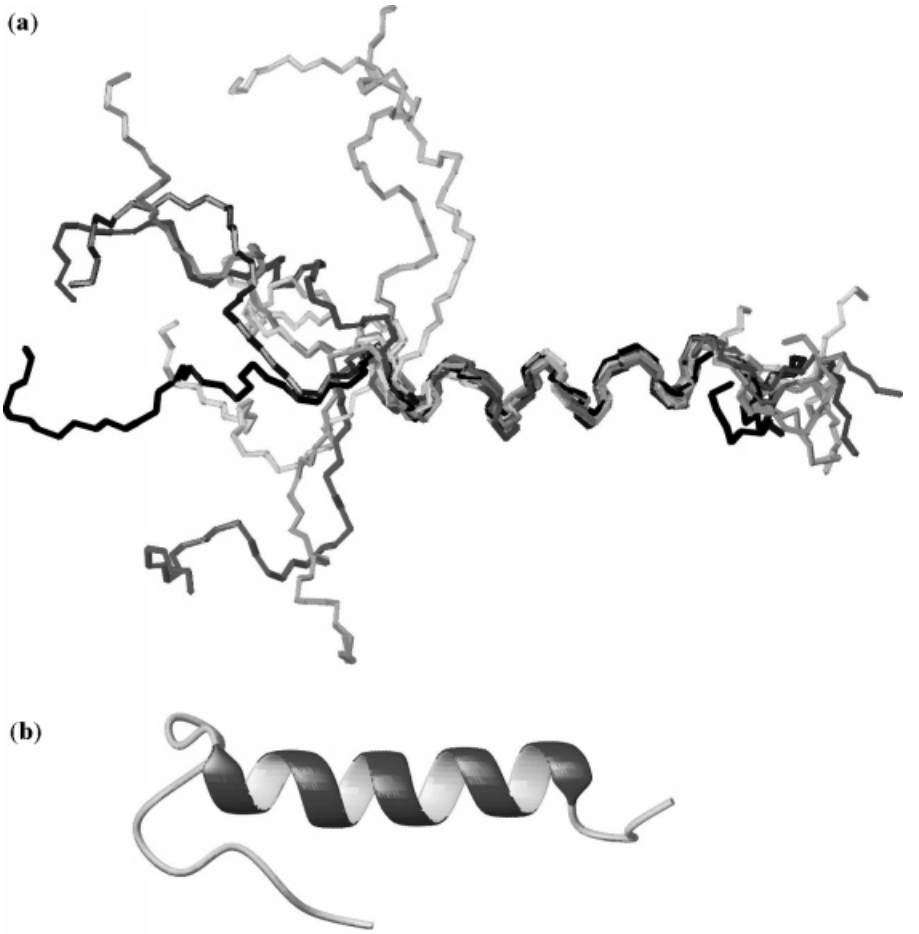

Figure 5 The NMR-derived solution structures of β-endorphin. (a) Superposition of the backbone N, C^{α} and C′ atoms of the ten final structures, refined by cartesian space restrained MD simulated annealing, with no violation greater than 0.5 Å in distance restraints for the helical segment. The *N*-terminal first 12 residues and the *C*-terminal last four residues are highly disordered. (b) Ribbon representation of the best structure of β-endorphin generated using MOLMOL.

coefficients and exchange rates of amide protons of model helical peptides in a mixture of trifluoroethanol and water demonstrated that H/D exchange is potentially more informative than temperature coefficients even for small peptides [61]. In spite of the relatively small size of β-endorphin, it was indeed possible to observe differential hydrogen deuterium exchange when the peptide was dissolved in deuterated HFA mixed with D_2O (50:50, v/v). In particular, the resonances of L^{17}, A^{21}, I^{22}, I^{23} and K^{24}, showed half-lives of up to 12 h as can be appreciated by inspection of Figure 4; the assignments of the peaks shown in the 1D spectra were obtained from short NOESY spectra. Such a behavior indicates a remarkable stability of the helix even in the absence of a tertiary structure.

Introduction of restraints corresponding to only two intramolecular hydrogen bonds (those involving residues A^{21}–L^{17} and I^{22}–F^{18}) in the DYANA torsion angle dynamics (TAD) procedure yielded a very regular α-helix from Pro^{13} to Tyr^{27}. In order to improve the quality of the structure determination we resorted first to restrained MM and finally to restrained MD simulated annealings on the ten best structures generated by DYANA. Both restrained MM and restrained MD procedures led to improvements in the quality of molecular parameters, as judged from deviations from idealized covalent geometry and from canonical ϕ, ψ pairs of the torsion angles, although to the expense of slight increases in restraint violations. We chose the adherence to idealized Ramachandran distribution as a satisfactory

criterion of structure quality. Table 2 summarizes the relevant statistics of the structure determination procedures. Figure 5a shows the molecular models of the ten structures of β-endorphin corresponding to the best structures calculated by DYANA and refined by means of restrained simulated annealing. Figure 5b shows the ribbon representation of the best structure of β-endorphin generated using MOLMOL; the peptide backbone torsion angles corresponding to the structure of Figure 5b are reported in Table 3.

DISCUSSION

The results of our conformational analysis show that human β-endorphin has very little tendency to assume an ordered structure in water but a strong tendency to assume a helical structure in its address domain (from P^{13} to Y^{27}) in apolar microenvironments, such as those assured by mixtures of water and alcohols, particularly in TFE/water (30:70, v/v) and HFA/water (50:50, v/v). In fact, according to Rajan *et al.* [58], a HFA/water mixture may be able to surround the helix with a sort of 'teflon coating'.

Table 3 Backbone Dihedral Angles of the Best Structure Calculated by AMBER

Residue	ϕ	ψ
Tyr^{1}		139.999
Gly^{2}	−51.224	−36.643
Gly^{3}	−54.305	−31.303
Phe^{4}	−77.976	58.821
Met^{5}	−76.652	58.909
Thr^{6}	−82.599	30.457
Ser^{7}	−75.812	71.649
Glu^{8}	−49.334	−52.127
Lys^{9}	−148.492	148.191
Ser^{10}	−157.224	54.804
Gln^{11}	−95.138	−119.677
Thr^{12}	−150.454	147.795
Pro^{13}	−51.013	
Leu^{14}	−48.476	−28.939
Val^{15}	−36.554	−41.410
Thr^{16}	−54.168	−51.673
Leu^{17}	−69.386	−44.733
Phe^{18}	−54.439	−44.342
Lys^{19}	−60.620	−60.513
Asn^{20}	−38.934	−45.902
Ala^{21}	−53.891	−35.287
Ile^{22}	−71.384	−50.022
Ile^{23}	−52.994	−41.427
Lys^{24}	−42.865	−44.218
Asn^{25}	−49.547	−42.402
Ala^{26}	−58.279	−26.782
Tyr^{27}	−83.698	−4.180
Lys^{28}	−78.638	54.663
Lys^{29}	−84.029	−52.633
Gly^{30}	69.803	−76.831
Glu^{31}	−87.391	

Many structural studies on medium sized peptides in these mixtures are performed on short sequences extracted from protein structures to test their intrinsic ability to keep the same secondary structure adopted in the protein [57,62]. It seems natural to think that the tendency to form helical segments depends both on the sequence of the peptide and on the property of the solvent to create a favorable environment but it is usually very difficult to untangle the two effects. Accordingly, the only parameter by which to judge the conformational tendencies of a fragment is to compare the length of the helical stretch found in solution with that present in the protein. In this respect, we wish to emphasize that the structure of β-endorphin yields an interesting example of an internal probe for the tendency of given amino acid sequences to form helical structures in helicogenic solvents. The finding that only half of the molecule assumes a very regular helical conformation, whereas the *N*-terminal dodecapeptide moiety remains disordered, hints that the role of the sequence is prevailing in this case. On the other hand, β-endorphin, although processed *in vivo* from a larger protein, is not just a fragment but a peptide hormone with a well-defined biological activity and its own structure–activity relationship. Thus, the nature and location of the secondary structure elements one eventually finds may reveal something on the function of each segment. In other words, the fact that the initial 12 amino acids do not show any tendency to go helical even in a strong helix-inducing solvent as HFA/water (50:50, v/v) hints that the *N*-terminal message domain must remain very flexible to favor an induced fit with the receptor active site, whereas the *C*-terminal address domain can assume a regular helical structure that favors an interaction with stable elements of secondary structure of the apolar cavity of the receptor. Strictly speaking, the solvent we used (HFA/water (50:50, v/v)) is not an apolar medium but it has been claimed [58] that it can effectively shield apolar side chains from water.

It is interesting to examine this hypothesis also from the point of view of sequence analysis. The

```
                          *****.   *:.: **:***:*.::*. : *
human (P01189)            YGGFMT--SEKSQTPLVTLFKNAIIKNAY-KKGE
macaca (P01201)           YGGFMT--SEKSQTPLVTLFKNAIIKNAY-KKGQ
elephant (P21252)         YGGFMT--SEKSQTPLVTLFKNAIIKNAY-KKG-
bovin (M25587)            YGGFMT--SEKSQTPLVTLFKNAIIKNAH-KKGQ
mouse (P01193)            YGGFMT--SEKSQTPLVTLFKNAIIKNAH-KKGQ
vison (P11280)            YGGFMT--SEKSQTPLVTLFKNAIIKNAH-KKGQ
pig (P01195)              YGGFMT--SEKSQTPLVTLFKNAIVKNAH-KKGQ
whale (P01195)            YGGFMT--SEKSZTPLITLFKNAIIKNAH-KKGQ
rat (P01194)              YGGFMT--SEKSQTPLVTLFKNAIIKNVH-KKGQ
guinea pig (P19402)       YGGFMS--SEKSQTPLVTLFKNAIVKNAH-KKGQ
frog (P22923)             YGGFMT--PERSQTPLMTLFKNAIIKNAH-KKGQ
bullfrog (P11885)         YGGFMT--PERSQTPLMTLFKNAIIKNAH-KKGQ
dog (A61167)              YGGFMS--SERSQTPLVTLFKNAIVKNAH-KK--
xenopus (P06299)          YGGFMT--PERSQTPLMTLFKNAIIKNSH-KKGQ
ostrich (A61326)          YGGFMS--SERGRAPLVTLFKNAIVKSAY-KKGQ
lungfish (P41589)         YGGFMKSWDERSQKPLMTLFKNVMIKDAYEKKGQ
longnose gar (U59910)     YGGFMKSWDERSQKPLLTLFKNVIIKDGHQKKGQ
white sturgeon (P87352)   YGGFMKSWDERSQKPLLTLFKNVMIKDGHEKKGQ
salmon (Q04618)           YGGFMKSWDERSQKPLLTLFKNVIIKDGQQKRE-
squalus acant. (P01197)   YGGFMKSWDERGQKPLLTLFRNVIVKDGHEK--
```

Figure 6 Alignment of 20 sequences of β-endorphin from different species. The alignment was obtained with ClustalW. The header shows the symbols for 100% identity (*) or similarity (: or .) used by this program. The order of the sequences corresponds to the output of BLAST2. The most conserved segments, corresponding to the Met-enkephalin sequence (YGGFM) and to the helical part of the address domain (PLVTLFKNAIIKNAY) are boxed.

sequence of β-endorphin is highly conserved among different species. Figure 6 shows the alignment of 20 sequences of β-endorphin from different species, as yielded by ClustalW [63]. The header shows the symbols for 100% identity (*) or similarity (: or .) used by this program. The order of the sequences corresponds to the output of BLAST2 [64] and reflects a decreasing similarity, also with respect to evolutionary distance. It can be seen that the *N*-terminal sequence, coincident with Met-enkephalin, is common to all species as required by the opioid activity. In addition, the central helical segment, spanning from P^{13} to Y^{27} in human β-endorphin, is highly conserved, with only a few homologous mutations and the conservation, *in all species*, of the initial residue of the helix (P^{13} in human β-endorphin). The majority of mutations are concentrated in the last four residues of the *C*-terminal part, beyond the helical segment, and in the linker region between the initial enkephalin sequence and the helical segment (T^{6}SEKSQT^{12}). In fact, the probability of forming helical segments, as predicted by methods based on the use of neural networks such as PHD [65], shows that even the least related sequences have a very similar intrinsic tendency, e.g. the prediction of helicity for human β-endorphin and for the corresponding peptide of Squalus acanthias yields the same length of α-helix for the corresponding segments P^{13}–Y^{27} and P^{15}–H^{29}, respectively.

The intrinsic tendency of the *C*-terminal part of the sequence to assume a very regular helical structure in an apolar micro-environment [58] suggests possible mechanisms of interaction of β-endorphin with the 7TM helices opioid receptors. It seems reasonable to hypothesize a 'two-point' attachment involving an interaction of the helical part of β-endorphin (the address domain) with either an extracellular loop or with one or more of the transmembrane helices and the (triggering) interaction of the message domain (YGGF) with the receptor subsite common to all opioid receptors. Most existing models of 7TM helices receptors do not suggest any structure for either extracellular or cytosolic loops. Accordingly, it is nearly impossible to propose a model for the interaction with extracellular loops. On the other hand, it may be possible to formulate an explicit model for the interaction of the P^{13}–Y^{27} helix with one or more of the TM helices of the opioid receptors. Figure 7 shows a schematic model of the μ receptor hosting the helical segment of β-endorphin. The μ model is represented by the extracellular view of the uppermost seven residues of the seven transmembrane helices, adapted from a schematic model of the web site of the University of Minnesota (http://www.opioid.umn.edu). However, the numbering of the TM helices residues and their relative orientation is that of Pogozheva *et al.* [35]. The only criteria used to pack the helix of β-endorphin were

the choice of the TM helices most likely to interact with the peptide, the importance of the interaction among helical dipoles in a strongly apolar environment, the need of leaving sufficient room for the interacting of the message domain and the favorable interaction of basic residues with the negative membrane surface. All these considerations lead to the model of Figure 7 in which the helix of endorphin interacts with all five helices that contribute most in forming the active site (**III**, **IV**, **V**, **VI** and **VII**). The helix of the peptide is both antiparallel to helices **III**, **V** and **VII** and places residues K28 and K29 on the surface of the membrane. The lateral orientation of the β-endorphin helix was qualitatively optimized by taking into account the distribution of residues. It is more difficult to evaluate the room left for a good interaction with the active site since this depends critically on the angle formed by the axis of the endorphin helix with the corresponding axes of the TM helices but it is certainly possible to put the relevant pharmacophores of endorphin close to the hypothesized residues [35] if the message adopts a folded conformation.

One interesting point connected with the interaction of the P^{13}–Y^{27} segment with TM helices is the complete absence of helicity of other parts of the sequence of β-endorphin even in strong helicogenic environments. The lack of helical structure in the first five residues, corresponding to the sequence of Met-enkephalin, although at variance with the early claim of Lichtarge *et al.* [33], is not surprising since enkephalin is known to be extremely flexible [21] but the total lack of helicity in the T^{6}–T^{12} segment is more surprising. In fact, in the sequence of

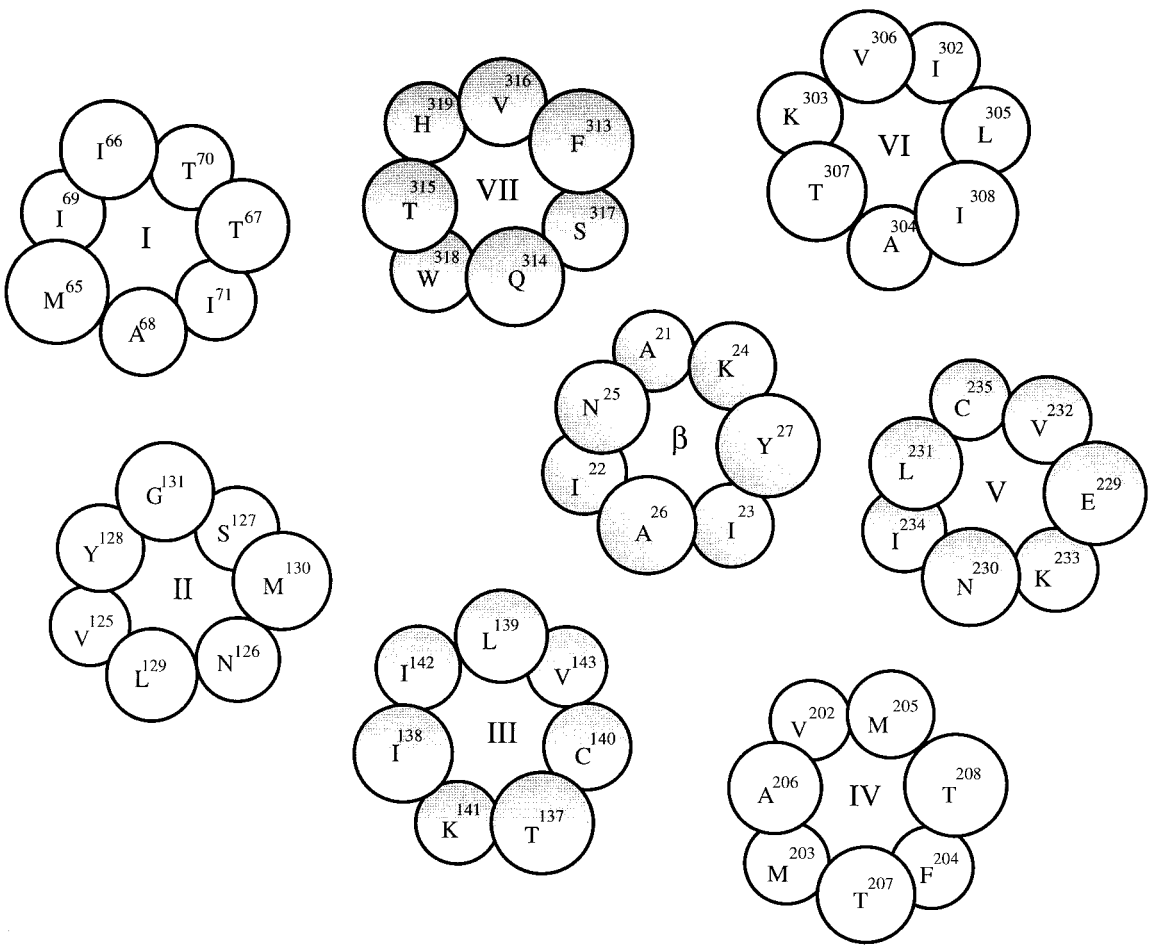

Figure 7 Schematic model of the μ receptor hosting the helical segment of β-endorphin. The μ model is represented by the extracellular view of the uppermost seven residues of the seven transmembrane helices. The helices are labeled with roman numerals (**I**–**VII**) whereas the helical segment of β-endorphin is labeled with a β. The helices that are thought to interact more strongly are highlighted with gray shading.

β-endorphin, there are potential Ncap [66] and Ccap motifs [67]: two Ncap sequences corresponding to variations of the classical SXXE box, S^7EKS^{10} and E^8KSQ^{11}, and a single (albeit trivial) Ccap sequence, $NAYKKG^{30}E$, coinciding with the physical end of the peptide.

Accordingly one might expect a single helical segment extending from S^7 to Y^{27}. It might be argued that P^{13} can act as an effective helix-breaker but this residue is not really incompatible with helices [68], it can simply produce a kink in a helix extending from S^7 to Y^{27}. This type of behavior is well documented in several helical peptides [69] and it has been specifically observed that a unique feature of TM helices is an apparently higher content of Pro [70]. It is interesting to observe that formation of a helical segment in the sequence $T^6SEKSQT^{12}$, although compatible with some predictions [25,27,66,67], would lead to unfavorable interactions inside the receptor. That is, a helix with even a partially polar surface could not interact well with the very hydrophobic surfaces of the TM helices. On the other hand, each residue of the linker region ($M^6TSEKSQT^{12}$) can easily interact with the few polar residues of TM helices of the active site (**III**, **IV**, **V**, **VI** and **VII**) if not forced to stay on a helical surface. That is, formation of a helix between residues P^{13} and Y^{27} seems consistent with the hypothesis of a direct interaction of the address message of β-endorphin with a TM helix of the receptor, whereas the message domain (Y^1GGF^4) and the linker region ($M^6TSEKSQT^{12}$) would assume a conformation induced by the shape of the receptor cavity.

Acknowledgements

The support of the CIMCF of the University of Naples for NMR measuring time is gratefully acknowledged. P.A.T. thanks Dr Annalisa Pastore and Dr Franca Fraternali (NIMR, MRC, Mill Hill, London, UK) for very helpful discussions and constant encouragement.

REFERENCES

1. Li CH. Lipotropin, a new active peptide from pituitary glands. *Nature* 1964; **201**: 924.
2. Li CH. beta-Endorphin. *Cell* 1982; **31**: 504–505.
3. Takahashi H, Teranishi Y, Nakanishi S, Numa S. Isolation and structural organization of the human corticotropin–beta-lipotropin precursor gene. *FEBS Lett.* 1981; **135**: 97–102.
4. Schwyzer R. Estimated conformation, orientation, and accumulation of dynorphin A-(1–13)-tridecapeptide on the surface of neutral lipid membranes. *Biochemistry* 1986; **25**: 6335–6342.
5. Hruby VJ, Gehrig CA. Recent developments in the design of receptor specific opioid peptides *Med. Res. Rev.* 1989; **9**: 343–401.
6. Hughes J, Smith TW, Kosterlitz HW, Fothergill LA, Morgan BA, Morris R. Identification of two related pentapeptides from the brain with potent opiate agonist activity. *Nature* 1975; **258**: 577–579
7. Goldstein A, Tachibana S, Lownej LI, Hunkapiller M, Hood L. Dynorphin-(1–13), an extraordinarily potent opioid peptide. *Proc. Natl. Acad. Sci. USA* 1979; **76**: 6666–6670.
8. Brantl V. Novel opioid peptides derived from human beta-casein: human beta-casomorphins. *Eur. J. Pharmacol.* 1984; **106**: 213–214.
9. Zadina JE, Hackler L, Ge LJ, Kastin AJ. A potent and selective endogenous agonist for the μ-opiate receptor. *Nature* 1997; **386**: 499–502.
10. Erspamer V. The opioid peptides of the amphibian skin. *Int. J. Dev. Neurosci.* 1992; **10**: 3–30.
11. Raynor K, Kong H, Chen Y, Yasuda K, Yu L, Bell GI, Reisine T. Pharmacological characterization of the cloned kappa-, delta-, and mu-opioid receptors. *Mol. Pharmacol.* 1994; **45**: 330–334.
12. Simon EJ. Opiate receptors and opioid peptides: an overview. *Ann. N. Y. Acad. Sci.* 1982; **398**: 327–339.
13. Kosterlitz HW. *The Wellcome Foundation Lecture*, 1982. Opioid peptides and their receptors. *Proc. R. Soc. London* 1985; **225**: 27–40.
14. Wuster M, Schulz R, Herz A. Specificity of opioids towards the mu-, delta- and epsilon-opiate receptors. *Neurosci. Lett.* 1979; **15**: 193–198.
15. Wuster M, Schulz R, Herz A. The direction of opioid agonists towards mu-, delta- and epsilon-receptors in the vas deferens of the mouse and the rat. *Life Sci.* 1980; **27**: 163–170.
16. Schulz R, Wuster M, Herz A. Pharmacological characterization of the epsilon-opiate receptor. *J. Pharmacol. Exp. Ther.* 1981; **216**: 604-606.
17. Nock B, Giordano AL, Moore BW, Cicero TJ. Properties of the putative epsilon opioid receptor: identification in rat, guinea pig, cow, pig and chicken brain. *J. Pharmacol. Exp. Ther.* 1993; **264**: 349–359.
18. Reisine T. Opiate receptors. *Neuropharmacology* 1995; **34**: 463–472.
19. D'Souza MM, Carr JA. Characterization of [125I]beta-endorphin binding sites in the rat caudal dorsomedial medulla. *Peptides* 1998; **19**, 931–937
20. Bond C, LaForge KS, Tian M, Melia D, Zhang S, Borg L, Gong J, Schluger J, Strong JA, Leal SM, Tischfield JA, Kreek MJ, Yu L. Single-nucleotide polymorphism in the human mu opioid receptor gene alters

beta-endorphin binding and activity: possible implications for opiate addiction. *Proc. Natl. Acad. Sci. USA* 1998; **95**: 9608–9613

21. Amodeo P, Naider F, Picone D, Tancredi T, Temussi PA. Conformational sampling of bioactive conformers: a low temperature NMR study of 15*N*-Leu-enkephalin. *J. Peptide Sci.* 1998; **44**; 253–265.
22. Chakrabarti S, Law PY, Loh HH. Distinct differences between morphine- and [D-Ala2,*N*-MePhe4,Gly-ol5]-enkephalin-mu-opioid receptor complexes demonstrated by cyclic AMP-dependent protein kinase phosphorylation. *J. Neurochem.* 1998; **71**: 231–239.
23. Hollosi M, Kajtar M Graf L. Studies on the conformation of beta-endorphin and its constituent fragments in water and trifluorethanol by CD spectroscopy. *FEBS Lett.* 1977; **74**: 185–189.
24. Yang JT, Bewley TA, Chen GC, Li CH. Conformation of beta-endorphin and beta-lipotropin: formation of helical structure in methanol and sodium dodecyl sulfate solutions. *Proc. Natl. Acad. Sci. USA* 1977; **4**: 3235–3238.
25. Jibson MD, Li CH. beta-Endorphin. Circular dichroism of synthetic human analogs with various chain lengths in methanol solutions. *Int. J. Peptide Protein Res.* 1981; **18**: 297–301.
26. Graf L, Hollosi M, Barna I, Hermann I, Borvendeg J, Ling N. Probing the biologically and immunologically active conformation of beta-endorphin: studies on C-terminal deletion analogs. *Biochem. Biophys. Res. Commun.* 1980; **95**: 1623–1627
27. Wu CCS, Lee NM, Loh HH, Yang JT, Li CH. beta-Endorphin: formation of alpha-helix in lipid solutions. *Proc. Natl. Acad. Sci. USA* 1979; **76**: 3656–3659.
28. Cabassi F, Zetta L. Human beta-endorphin. 270-MHz 1H-nuclear-magnetic-resonance study of glycyl-residues in aqueous solution. *Int. J. Peptide Protein Res.* 1982; **20**: 154–158.
29. Zetta L, Kaptein R. Interaction of beta-endorphin with sodium dodecyl sulfate in aqueous solution. 1H-NMR investigation. *Eur. J. Biochem.* 1984; **145**: 181–186
30. Zetta L, Hore PJ, Kaptein R. Investigation by photochemically-induced dynamic nuclear polarization and nuclear overhauser enhancement ^{1}H-NMR of the interaction between β-endorphin and phospholipid micelles. *Eur. J. Biochem.* 1983; **134**; 371–376.
31. Zetta L, De Marco A, Vecchio G, Gazzola G, Longhi R. In *Protides of the Biological Fluids*, vol. 35. Pergamon Press, 1987; 461–464.
32. Zetta L, Consonni R, De Marco A, Longhi R, Manera E, Vecchio G. Opioid peptides in micellar systems: conformational analysis by CD and by one-dimensional and two-dimensional 1H-NMR spectroscopy. *Biopolymers* 1990; **30**: 899–909
33. Lichtarge O, Jardetzky O, Li CH. Secondary structure determination of human beta-endorphin by 1H NMR spectroscopy. *Biochemistry* 1987; **26**: 5916–5925.
34. Deschamps JR, George C, Flippen-Anderson JL. Structural studies of opioid peptides: a review of recent progress in X-ray diffraction studies. *Biopolymers (Peptide Sci.)* 1996; **40**: 121–139.
35. Pogozheva, ID, Lomize AL, Mosberg H. Opioid receptor three-dimensional structures from distance geometry calculations with hydrogen bonding constraints. *Biophys. J.* 1998; **75**: 612–634.
36. Wüthrich K. In *NMR of Proteins and Nucleic Acids*. Wiley: New York, 1986; 162–175.
37. Piantini U, Soerensen OW, Ernst RR. Multiple quantum filters for elucidating NMR coupling networks. *J. Am. Chem. Soc.* 1982; **104**: 6800–6801.
38. Bax A, Davis DG. Mlev-17-based two-dimensional homonuclear magnetization transfer spectroscopy. *J. Magn. Reson.* 1985; **65**: 355–360.
39. Jeener J, Meyer BH, Bachman P, Ernst RR. Investigation of exchange processes by two-dimensional nmr spectroscopy. *J. Chem. Phys.* 1979; **71**: 4546–4553.
40. Levitt MH, Freeman R, Frenkiel T. Broadband heteronuclear decoupling. *J. Magn. Reson.* 1982; **47**: 328–330.
41. Marion D, Wüthrich, K. Application of phase sensitive two-dimensional correlated spectroscopy (COSY) for measurements of 1H-1H spin-spin coupling constants in proteins. *Biochem. Biophys. Res. Commun.* 1983; **113**: 967–971.
42. Piotto M, Saudek V, Sklenar V. Gradient-tailored excitation for single-quantum NMR spectroscopy of aqueous solutions. *J. Biomol. NMR* 1992; **2**: 661–666.
43. Güntert P, Mumenthaler C, Wüthrich K. Torsion angle dynamics for NMR structure calculation with the new program DYANA. *J. Mol. Biol.* 1997; **273**: 283–298.
44. Weiner SJ, Kollman PA, Nguyen DT, Case DA. An all-atom force-field for simulations of proteins and nucleic acids. *J. Comp. Chem.* 1986; **7**: 230–252.
45. Pearlman DA, Case DA, Caldwell JW, Ross WS, Cheatham III TE, DeBolt S, Ferguson D, Seibel G, Kollman PA. AMBER, a computer program for applying molecular mechanics, normal mode analysis, molecular dynamics and free energy calculations to elucidate the structures and energies of molecules. *Comp. Phys. Commun.* 1995; **91**: 1–41.
46. Berendsen HJC, Postma JPM, van Gunsteren WF, DiNola A, Haak JR. Molecular dynamics with coupling to an external bath. *J. Chem. Phys.* 1984; **81**: 3684–3690.
47. Koradi R, Billeter M, Wüthrich K. MOLMOL: a program for display and analysis of macromolecular structures. *J. Mol. Graph.* 1996; **14**: 51–55.
48. Temussi PA, Amodeo P, Picone D, Tancredi T. Solution structure of bioactive peptides in biomimetic media. *Acta Pharm.* 1992; **42**: 323–328.
49. Temussi PA. NMR studies of flexible bioactive peptides. In *Encyclopedia of NMR*. J. Wiley and Sons: New York, 1996.

50. D'Ursi A, Albrizio S, Tancredi T, Temussi PA. Environmental constraints in the study of flexible segments of proteins. *J. Biomol. NMR* 1998; **11**: 1–8.
51. Douzou P, Petsko GA. Proteins at work: 'Stop-Action' pictures at subzero temperatures. *Adv. Protein Chem.* 1984; **36**: 245–261.
52. Amodeo P, Motta A, Picone D, Saviano G, Tancredi T, Temussi PA. Viscosity as a conformational sieve. Noe of linear peptides in cryoprotective mixtures. *J. Magn. Reson.* 1991; **95**: 201–207.
53. Bazzo R, Tappin MJ, Pastore A, Harvey TS, Carver JA, Campbell ID. The structure of melittin. A 1H-NMR study in methanol. *Eur. J. Biochem.* 1988; **173**: 139–146.
54. Marion D, Zasloff M, Bax A. A two-dimensional NMR study of the antimicrobial peptide magainin 2. *FEBS Lett.* 1988; **227**: 21–26.
55. Sonnichsen FD, Van Eyk JE, Hodges RS, Sykes BD. Effect of trifluoroethanol on protein secondary structure: an NMR and CD study using a synthetic actin peptide. *Biochemistry* 1992; **31**: 8790–8798
56. Verheyden P, De Wolf E, Jaspers H, Van Binst G. Comparing conformations at low temperature and at high viscosity. Conformational study of somatostatin and two of its analogues in methanol and in ethylene glycol. *Int. J. Peptide Protein Res.* 1994; **44**, 401–409
57. Reymond MT, Huo S, Duggan B, Wright PE, Dyson HJ. Contribution of increased length and intact capping sequences to the conformational preference for helix in a 31-residue peptide from the C terminus of myohemerythrin. *Biochemistry* 1997; **36**: 5234–5244
58. Rajan R, Awasthi SK, Bhattachajya S, Balaram P. Teflon-coated peptides: hexafluoroacetone trihydrate as a structure stabilizer for peptides. *Biopolymers* 1997; **42**: 125–128.
59. Picone D, D'Ursi A, Motta A, Tancredi T, Temussi PA. Conformational preferences of [Leu5]enkephalin in biomimetic media. Investigation by 1H NMR. *Eur. J. Biochem.* 1990; **192**: 433–439.
60. Kim Y, Prestegard JH. Measurement of vicinal coupling from cross peaks in COSY spectra. *J. Magn. Reson.* 1989; **84**: 9–13.
61. Rothemund S, Weisshoff H, Beyermann M, Krause E, Bienert M, Mugge C, Sykes BD, Sonnichsen FD. Temperature coefficients of amide proton NMR resonance frequencies in trifluoroethanol: a monitor of intramolecular hydrogen bonds in helical peptides. *J. Biomol. NMR* 1996; **8**: 93–97.
62. Ramirez-Alvarado M, Serrano L, Blanco FJ. Conformational analysis of peptides corresponding to all the secondary structure elements of protein L B1 domain: secondary structure propensities are not conserved in proteins with the same fold. *Protein Sci.* 1997; **6**: 162–174.
63. Thompson JD, Higgins DG, Gibson TJ. CLUSTAL W: improving the sensitivity of progressive multiple sequence alignment through sequence weighting, position-specific gap penalties and weight matrix choice. *Nucleic Acids Res.* 1994; **22**: 4673–4680.
64. Altschul SF, Gish W, Miller W, Myers EW, Lipman DJ. Basic local alignment search tool. *J. Mol. Biol.* 1990; **215**: 403–410.
65. Rost B, Sander C. Prediction of protein secondary structure at better than 70% accuracy. *J. Mol. Biol.* 1993; **232**: 584–599.
66. Harper ET, Rose GD. Helix stop signals in proteins and peptides: the capping box. *Biochemistry* 1993; **32**: 7605–7609.
67. Aurora R, Srinivasan R, Rose GD. Rules for α-helix termination by glycine. *Science* 1994; **264**: 1126–1130.
68. Swindells MB, MacArthur MW, Thornton JM. Intrinsic phi, psi propensities of amino acids, derived from the coil regions of known structures. *Nat. Struc. Biol.* 1995; **2**: 596–603.
69. Biggin PC, Breed J, Son HS, Sansom MS. Simulation studies of alamethicin–bilayer interactions. *Biophys. J.* 1997; **72**: 627–636.
70. Hong S, Ryu KS, Oh MS, Ji I, Ji TH. Roles of transmembrane prolines and proline-induced kinks of the lutropin/choriogonadotropin receptor. *J. Biol. Chem.* 1997; **272**: 4166–4171.

